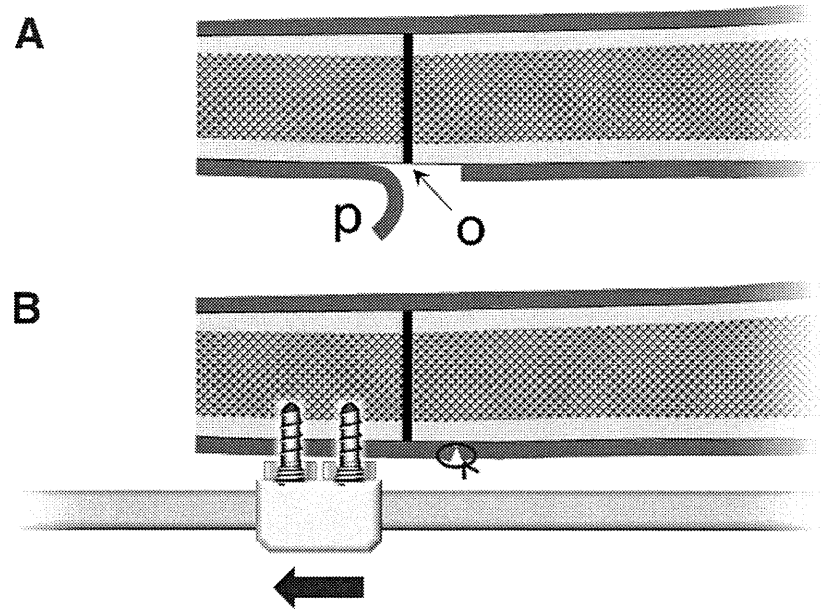

FIGURE 1. Preparation for supraperiosteal transport: o, osteotomy; p, periosteum. *A*, A minimal periosteal incision is made a few millimeters from a planned osteotomy line to create a transport segment; the periosteum is then reflected beyond the line. After the osteotomy, the periosteum is repositioned and sutured. *B*, The transport segment is supraperiosteally fixed with locking plates and screws of a distraction device. Unless they contain a locking mechanism, special care should be taken not to compress the underlying periosteum with plates, and fixation screws should not be fully tightened.

Hibi and Ueda. Supraperiosteal Transport Distraction Osteogenesis. J Oral Maxillofac Surg 2011.

traction mechanism of the device was detached to keep the remaining components of the device fully internal.

Computed tomograms (CTs) at 8 months after distraction showed that newly formed bone in the distraction gap progressed to continuous buccal and lingual cortical surfaces, allowing for secondary vertical DO to reconstruct the ascending ramus (Fig 2D). Using a subgonial approach, a periosteal cut and a horizontal osteotomy were performed buccally 8 and 9 mm from the superior edge of the transported segment, respectively. The 1-mm-long buccal periosteal flap of the secondary transport segment was repositioned and sutured, and a distraction device (Extension Plate System; Keisei Medical Industrial, Tokyo, Japan) was adjusted and fixed supraperiosteally with positioning screws (Center Drive 1.5; Gebrüder Martin, Tuttlingen, Germany; Fig 2E,F). After a 7-day latency period, the device was activated at a rate of 0.5 mm twice a day for 58 days until the secondary transport segment had reached the artificial condyle, when the distraction rod was cut to leave the remaining device fully internal. CTs at 9 months after the secondary distraction showed that newly formed bone in the distraction gap progressed to the continuous buccal and lingual cortical surfaces of the ascending ramus (Fig 2G). The remaining components of the devices were removed, and the superior end of the regenerated ramus was connected to the cut end of the preserved condylar segment with a lag screw and plate (Condylar Lag Screw Plate System; Stryker Leibinger). The plate was fixed supraperiosteally on the regenerated ramus with the locking screws (1.7 Locking Screw; Stryker Leibinger) instead of its original fixation screws, and the space around the connected bony surfaces was filled with autologous tissue-engineered osteogenic material[5] (Fig 2H). Fourteen months after the second distraction, 3 titanium screw-type implants, 3.5 mm in diameter and 15 mm in length (Astra Tech Implant System; Astra Tech, Mölndal, Sweden), were installed in the second premolar and molar regions of the regenerated mandibular body with buccal veneer bone grafted from the contralateral ramus because of a thin ridge (Fig 2I). Twenty-two months after the second distraction, all the osseointegrated implants were uncovered and connected with abutments, the uncovered mucosa was positioned apically, and the exposed buccal bony surface of the ridge was covered with mucosa grafted from the palate for vestibuloplasty. The plate and screws on the reconstructed ramus were removed, and the mandibular angle was adjusted with osteotomy and screw fixation in the angle region (Fig 2J). At the time of this writing, the patient has been orally rehabilitated with a provisional implant-supported prosthesis for more than 3 years (Fig 2K).

CASE 2: BILATERAL TRANSPORT DO FOR MANDIBULAR ANTERIOR BODIES

A 61-year-old woman had suffered from an ameloblastoma, which recurred for the fourth time in the mesial and distal borders of the sectioned mandible and the interpositioning iliac bone graft (Fig 3A). She underwent a mandibular segmental resection to remove it and distraction device fixation for its reconstruction through a submandibular approach. Bilateral transport segments were created in the right premolar and left retromolar regions of the remaining mandible in the same manner as Case 1, and the custom-made distraction device was adjusted (Fig 3B). The transport segments were supraperiosteally fixed with the locking plates and screws (Fig 3C,D). After a 7-day latency period, the device was activated at a rate of 0.5 mm twice a day for 41 and 33 days on the right and left side, respectively (Fig 3E), until the transport segments reached each other, at which point the bilateral percutaneous traction

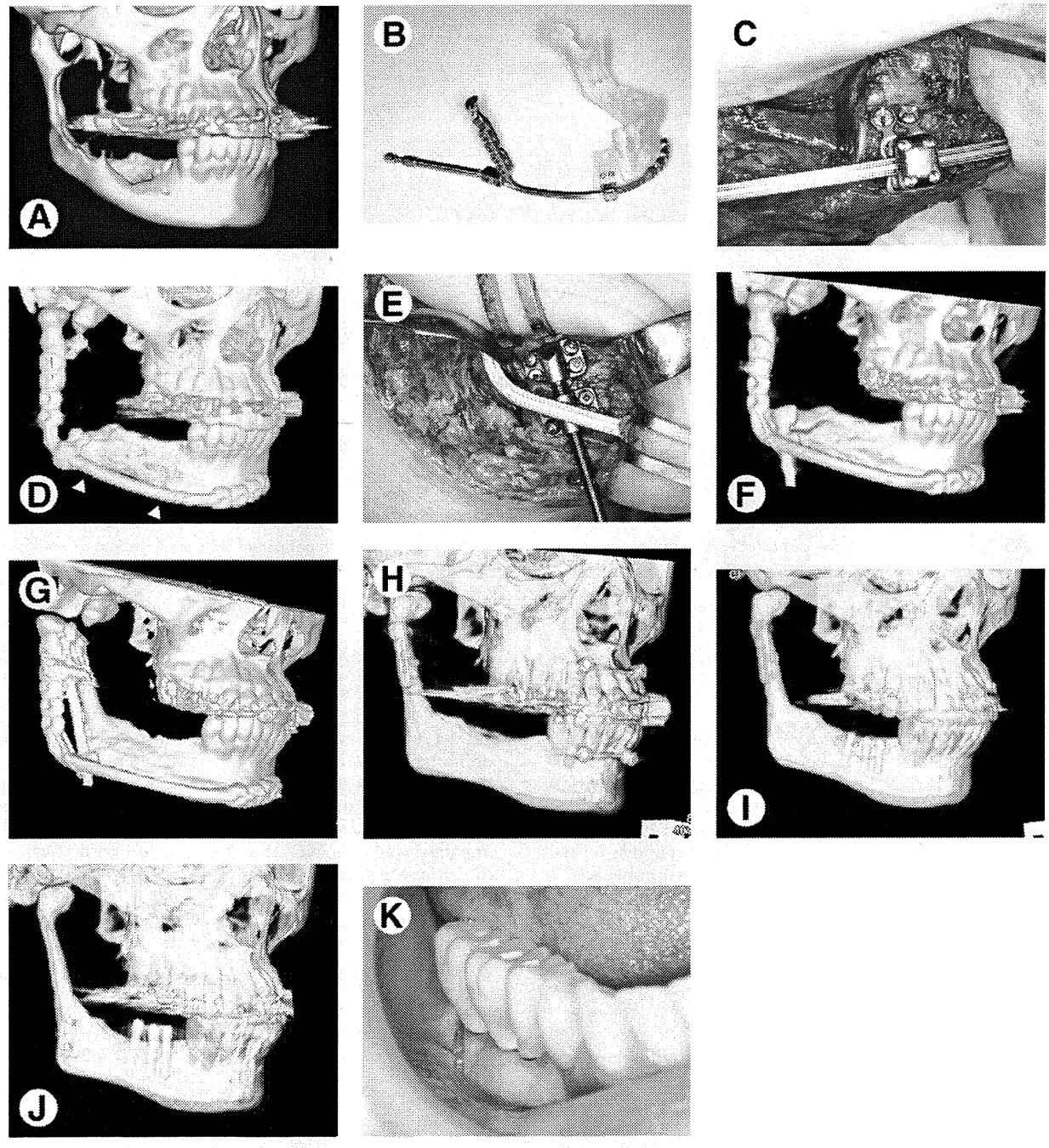

FIGURE 2. *A,* The mandible with a recurrent ameloblastoma. Computed tomography (CT) revealed a multilocular radiolucent image in the ramus and posterior body of the mandible. *B,* A custom-made distraction device with an artificial condyle on the patient's stereolithographic model. Locking plates and screws enabled supraperiosteal fixation of the transport segment. *C,* Supraperiosteal fixation of the distraction device. A short buccal periosteal flap of the transport segment was repositioned and sutured to cover the vertical osteotomy line. The transport segment was fixed with locking plates and screws supraperiosteally. *D,* The regenerated posterior mandibular body. Eight months after distraction, CT showed that newly formed 50-mm-long bone in the distraction gap (*arrowheads*) progressed to continuous buccal and lingual cortical surfaces. *E,* The secondary vertical distraction osteogenesis for reconstructing the ascending ramus. A short buccal periosteal flap of the secondary transport segment was repositioned and sutured to cover the horizontal osteotomy line. The transport segment was fixed with another distraction device and positioning screws supraperiosteally. *F,* Another transport segment. Immediately after surgery, CT showed the secondary transport segment fixed with the distraction device. *G,* The regenerated ascending ramus. Nine months after the secondary distraction, CT showed that newly formed bone in the distraction gap progressed to continuous buccal and lingual cortical surfaces of the ramus. *H,* Device removal and mandibular reconstruction. CT showed that the regenerated ramus is connected to the preserved condylar segment with a lag screw and plate. *I,* The regenerated mandibular body containing implants. CT showed 3 screw-type implants installed in the right second premolar and molar regions with a buccal veneer bone graft fixed with 2 screws. *J,* The reconstructed mandible and the osseointegrated implants for occlusal function. CT showed that the mandibular angle was adjusted with osteotomy and screw fixation in the angle region. *K,* A provisional implant-supported prosthesis on the reconstructed mandible. The ridge supporting the implants was surrounded by the attached mucosa, the buccal part of which originated from the palatal mucosa.

Hibi and Ueda. Supraperiosteal Transport Distraction Osteogenesis. J Oral Maxillofac Surg 2011.

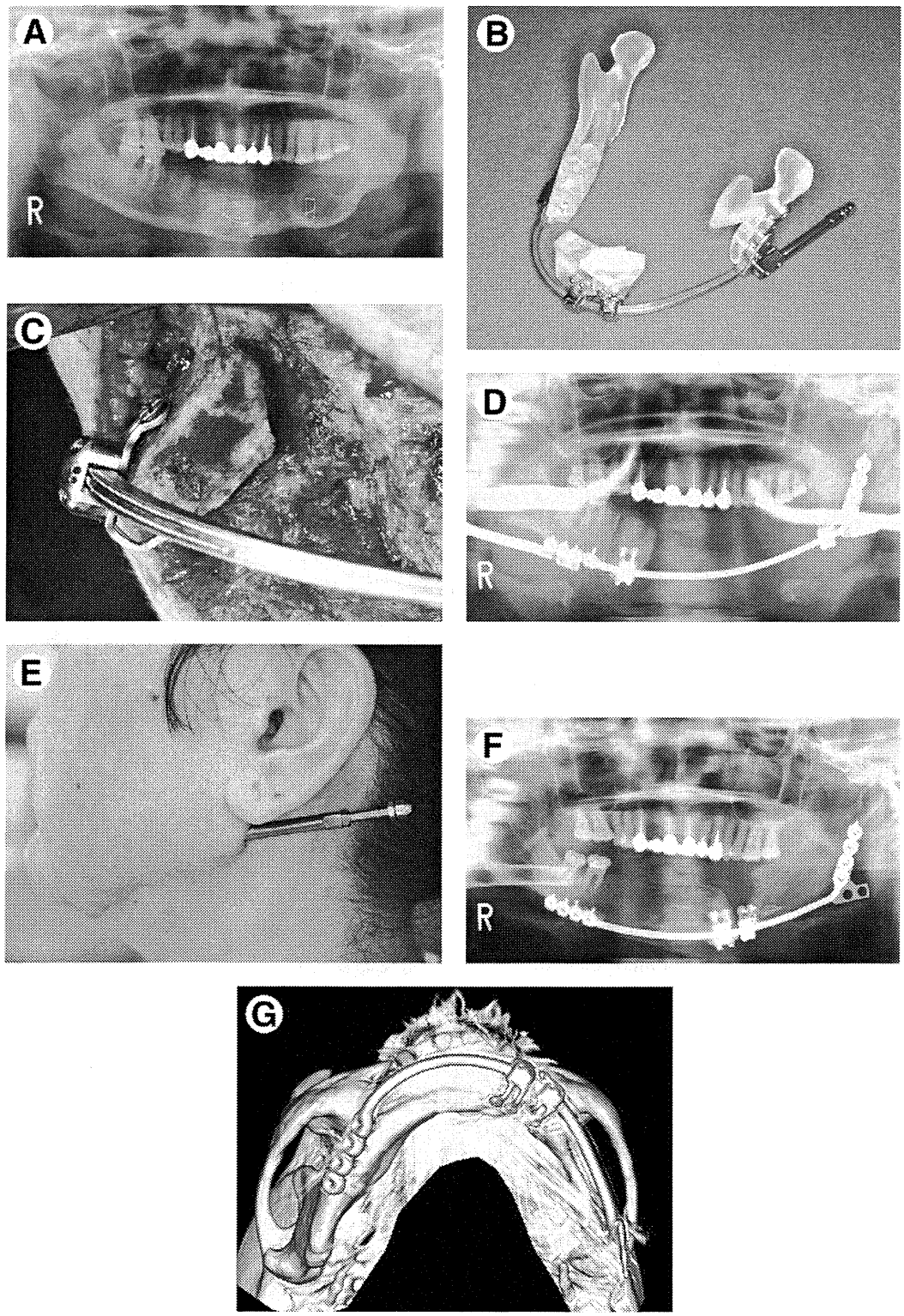

FIGURE 3. *A*, The mandible with a fourth recurrent ameloblastoma. Panoramic radiogram revealed radiolucent images in the mesial and distal borders of the sectioned mandible and the interpositioning iliac bone graft. *B*, A custom-made distraction device on the patient's stereolithographic model. Locking plates and screws enabled supraperiosteal fixation of the transport segments. *C*, The transport segment fixed with the locking plates and screws supraperiosteally. *D*, The transport segments before distraction. Immediately after surgery, panoramic radiogram showed the distraction device and 2 transport segments in their initial positions. *E*, The percutaneous traction mechanism of the distraction device. Activation of the mechanism moved the transport segment through a traction wire. *F*, Fourteen months after distraction, the panoramic radiogram showed newly formed bone with progressing density in the distraction gaps. *G*, Fourteen months after distraction, CT showed that newly formed bones in the distraction gaps, and the transport segments composed a multangular form resembling the mandibular curvature.

Hibi and Ueda. Supraperiosteal Transport Distraction Osteogenesis. J Oral Maxillofac Surg 2011.

mechanisms of the device were detached to keep the remaining components of the device fully internal. The panoramic radiogram and CTs at 14 months after distraction showed newly formed bones with progressing density in the distraction gaps, and the transport segments composed a multangular form resembling the mandibular curvature (Fig 3F,G). Detachment of the remaining components of the device and osteoplasty in the docking site of the transport segments are planned.

Discussion

Sufficient blood supply to the transport segment and DO site is important for appropriate new bone formation.[1,2] Periosteal attachment and continuity should therefore be maintained as much as possible. Without periosteal stripping, even internal distraction devices can be fixed supraperiosteally with fixation screws as positioning screws, as was done for the secondary distraction in Case 1. Although this technique may compress the periosteum under the plates or destabilize a distraction device, its effects can be decreased with modified plating and screwing. This situation can also be avoided with a locking plate and screw system, as shown in both cases. This system enables supraperiosteal application of the plates to be situated separately from bony surfaces. Commercially available distraction devices should contain a locking mechanism.

The periosteum should cover the distraction gap line because osteogenic cells are derived from bone marrow, the endosteum, and the periosteum. Even periosteal DO, which incorporates gradual periosteal elevation with customized devices without creating a bony transport segment, can lead to new bone formation in the subperiosteal spaces.[6-9] Periosteal DO in animal experiments as well as a human case of unintentional periosteal DO[10] have been reported. Subperiosteal new bone formation in the distraction gap can decrease postdistraction lateral concavity, which can present as fenestration or dehiscence defects; this is sometimes referred to as an hour-glass deformity.[11] Such deformity usually arises where the periosteum is cut and stripped off extensively to prepare bone cuts and seat a distraction device. In both the cases described here, clear cortical bony images without postdistraction lateral concavity were observed in the remodeling phase, with a minimally damaged periosteum.

In the maxillofacial region, in particular, alveolar DO uses smaller osteotomized transport segments, and preserving the periosteal attachment and periosteal coverage of the distraction gap line are critical factors in DO. Severe complications, such as fracture of the basal bone in vertical DO for edentulous mandibles and resorption of the transport segment, have been reviewed.[12] These effects can be attributed to interrupted blood supply to the complicated bone according to the area of the reflected periosteum. The concept of a supraperiosteal transport DO using the periosteal potential provides a solution for improving DO.

References

1. Ilizarov GA: The tension-stress effect on the genesis and growth of tissue. Part I. The influence of stability of fixation and soft-tissue preservation. Clin Orthop 238:249, 1989
2. Samchukov ML, Cope JB, Cherkashin AM: Basic principles of bone transport, *in* Samchukov, ML, Cope, JB, Cherkashin, AM (eds): Craniofacial Distraction Osteogenesis. St. Louis, MO, Mosby, 2001, pp 349-357
3. Hu J, Li J, Wang D, et al: Differences in mandibular distraction osteogenesis after corticotomy and osteotomy. Int J Oral Maxillofac Surg 31:185, 2002
4. Hibi H, Ueda M: New internal transport distraction device for reconstructing segmental defects of the mandible. Br J Oral Maxillofac Surg 44:382, 2006
5. Hibi H, Yamada Y, Ueda M, et al: Alveolar cleft osteoplasty using tissue-engineered osteogenic material. Int J Oral Maxillofac Surg 35:551, 2006
6. Schmidt BL, Kung L, Jones C, et al: Induced osteogenesis by periosteal distraction. J Oral Maxillofac Surg 60:1170, 2002
7. Kessler P, Bumiller L, Schlegel A, et al: Dynamic periosteal elevation. Br J Oral Maxillofac Surg 45:284, 2007
8. Estrada JIC, Saulacic N, Vazquez L, et al: Periosteal distraction osteogenesis: Preliminary experimental evaluation in rabbits and dogs. Br J Oral Maxillofac Surg 45:402, 2007
9. Sencimen M, Aydintug YS, Ortakoglu K, et al: Histomorphometrical analysis of new bone obtained by distraction osteogenesis and osteogenesis by periosteal distraction in rabbits. Int J Oral Maxillofac Surg 36:235, 2007
10. Hibi H, Nakai H, Tsurusako S, et al: A case of occlusal reconstruction using dental implants in revascularized scapular osteocutaneous flap [in Japanese]. J Jpn Soc Oral implant 22: 498, 2009
11. Garcia AG, Martin MS, Vila PG, et al: A preliminary morphologic classification of the alveolar ridge after distraction osteogenesis. J Oral Maxillofac Surg 62:563, 2004
12. Saulacic N, Zix J, Iizuka T: Complication rates and associated factors in alveolar distraction osteogenesis: A comprehensive review. Int J Oral Maxillofac Surg 38:210, 2009

Effects of Self-Assembling Peptide Hydrogel Scaffold on Bone Regeneration with Recombinant Human Bone Morphogenetic Protein-2

Masayuki Ikeno, DDS[1]/Hideharu Hibi, DDS, PhD[2]/Kazuhiko Kinoshita, DDS, PhD[1]/
Hisashi Hattori, DDS, PhD[3]/Minoru Ueda, DDS, PhD[4]

Purpose: *The objective of this pilot study was to histologically evaluate bone regeneration using a self-assembling peptide hydrogel scaffold with recombinant human bone morphogenetic protein-2 (rhBMP-2) in a rabbit calvaria model.* ***Materials and Methods:*** *Five adult New Zealand White rabbits were used for the study. Each received four titanium cylinders, which were placed into perforated slits made in the outer cortical bone of the calvaria. The cylinders were filled with the following test materials:* (1) *unfilled control;* (2) *rhBMP-2;* (3) *PuraMatrix (PM), a synthetic self-assembling peptide (RADA16-I) consisting of a 16-amino acid sequence and with a three-dimensional structure; and* (4) *PM/rhBMP-2. Each cylinder was covered with a titanium lid. After 8 weeks, the animals were sacrificed, and ground sections were obtained for histomorphometric analysis.* ***Results:*** *Histomorphometric analysis showed that regenerated tissue in the cylinder with PM/rhBMP-2 was significantly increased compared to the empty control. The mean area values of regenerated tissue in the cylinders were 35.80% ± 10.35% (control), 47.94% ± 5.65% (rhBMP-2), 48.94% ± 11.33% (PM), and 58.06% ± 14.84% (PM/rhBMP-2). The mean area values of newly formed bone in the cylinders were 9.39% ± 4.34% (control), 14.03% ± 2.25% (rhBMP-2), 13.99% ± 2.15% (PM), and 16.61% ± 3.79% (PM/rhBMP-2). Neither rhBMP-2 nor PM alone significantly enhanced bone regeneration compared to the empty control cylinder.* ***Conclusions:*** *PM with rhBMP-2 significantly enhanced bone regeneration on the bone augmentation model in a rabbit. PM promises to be a useful alternative synthetic material as a carrier for rhBMP-2 for bone regeneration.* Oral Craniofac Tissue Eng 2011;1:91–97

Key words: bone morphogenetic protein-2, bone regeneration, calvarial model, self-assembling peptide

[1]Researcher, Department of Oral and Maxillofacial Surgery, Nagoya University Graduate School of Medicine, Nagoya, Japan.
[2]Associate Professor, Department of Oral and Maxillofacial Surgery, Nagoya University Graduate School of Medicine, Nagoya, Japan.
[3]Lecturer, Department of Oral and Maxillofacial Surgery, Nagoya University Graduate School of Medicine, Nagoya, Japan.
[4]Professor, Department of Oral and Maxillofacial Surgery, Nagoya University Graduate School of Medicine, Nagoya, Japan.

Correspondence to: Hideharu Hibi, Department of Oral and Maxillofacial Surgery, Nagoya University Graduate School of Medicine, 65 Tsuruma-cho, Showa-ku, Nagoya 466-8550, Japan. Fax: +81-52-744-2352. Email: hibihi@med.nagoya-u.ac.jp

Bony defects in the craniofacial region resulting from tumor resection, trauma, congenital malformations, and periodontal disease are serious problems. The bone regeneration technique for bony defects has been widely accepted, and autologous bone grafts from the iliac crest and others are still the gold standard.[1,2] Although autologous bone grafts have excellent biologic and mechanical properties,[3] they may be associated with donor site morbidity or the available supply may be limited.[4] Various biomaterials have been tested as scaffolds for bone regeneration, such as beta-tricalcium phosphate, hydroxyapatite, and polymers.[5,6] However, a scaffold has still not been found that has the characteristics of biologic safety, absorbability, cell interaction, and bone inductivity.

A self-assembling peptide hydrogel scaffold is made of artificial synthetic materials featuring biologic safety and absorbability.[7,8] PuraMatrix (PM) is a synthetic self-assembling peptide (RADA16-I) that consists of a 16-amino acid sequence (AcN-RADARADARADARADA-CNH2) and more than 99.5% water (Fig 1).[7,8] PM has a three-dimensional structure, with fiber and pore sizes < 10 nm and 5 to 200 nm, respectively.[7,8] Bokhari et al reported that PM was a microcellular scaffold containing a nanoscale environment to enhance osteoblast differentiation and promote osteoblast growth in vitro.[9] It also has characteristics of fluidity, stickiness, and the plasticity needed for bony defects, and it turns into a gel upon contact with blood. Thus, PM is expected to be a candidate as a scaffold for bone regeneration.

A signal factor is required to induce osteogenesis.[10] Recombinant human bone morphogenetic protein-2 (rhBMP-2) has exhibited high osteogenic activity in experimental studies,[11] and the effects of rhBMP-2 in various carriers on bone regeneration have been reported.[12] Therefore, rhBMP-2 was used as a representative signal factor in this study.

The objective of this pilot study was to histologically evaluate bone regeneration using a self-assembling peptide hydrogel scaffold with rhBMP-2 on the bone augmentation in a rabbit calvaria model. This model has been used to estimate various bone substitutes for bone regeneration in recent years.[13–15]

MATERIALS AND METHODS

Animals

Five adult male New Zealand White rabbits weighing 3.2 to 3.5 kg were used. The animals were kept in individual cages and were fed a standard laboratory diet. General anesthesia was induced by combination of an intramuscular injection of xylazine (4 mg/kg body weight) and an intravenous injection of pentobarbital sodium (40 to 50 mg/kg body weight) through the ear vein. The experimental protocol was approved by the Animal Experiment Advisory Committee of Nagoya University School of Medicine and performed in accordance with the Guidelines for Animal Experimentation of Nagoya University.

Preparation of PM and rhBMP-2 Solution

PM (3-D Matrix Ltd) was prepared in vials at a peptide concentration of 10 mg/mL. The synthesis and characterization of PM were described previously.[16,17] PM was sonicated for 30 minutes in a bath sonicator (Yamato Chemical) and filtrated through a 0.22-μm sterile filter (Millipore) so it would flow uniformly. rhBMP-2 (Peprotech) was diluted in a 20% sucrose solution. Just before application, 50 μL of PM or saline, 50 μL of 20% sucrose solution with or without rhBMP-2, and 100 μL of phosphate-buffered saline (PBS) were mixed in the vial. The final concentration of rhBMP-2 amounted to 25 μg/mL.

Surgical Procedure

A midline incision was made from the nasal bone to the sagittal crest and a cutaneous flap was created. In the left and right parietal and frontal bones, four evenly distributed circular slits were prepared with a trephine drill (Technica) with an inner diameter of 6 mm and a depth of 1 mm. In the outer cortical bone inside this circle, five evenly distributed holes with a diameter of 1 mm each were prepared with a no. 2 round bur (Fig 2a). The experimental device was a custom-made cylinder of commercially pure titanium (> 99.5% titanium; SPF) with an inner diameter of 6 mm and height of 7 mm. The inside surface of each cylinder was machined titanium. After the bone surfaces of the calvaria were washed with saline to remove any bone powder, the apical end of each titanium cylinder was pressed into each of the slits (Fig 2b). Each animal received four cylinders, and the cylinders were randomly filled with the following: *(1)* unfilled control; *(2)* rhBMP-2 (50 μL of saline, 50 μL of 20% sucrose containing rhBMP-2, and 100 μL of PBS); *(3)* PM (50 μL of PM, 50 μL of 20% sucrose, and 100 μL of PBS); or *(4)* PM/rhBMP-2 (50 μL of PM, 50 μL of 20% sucrose containing rhBMP-2, and 100 μL of PBS) (Fig 2c). The top of the cylinders was covered with a titanium lid (Fig 2d). The flaps were adapted and sutured with 4-0 Vicryl (Ethicon) for primary healing. After 8 weeks, the animals were sacrificed and ground sections were obtained for histomorphometric analysis.

Histologic Preparation

Animals were sacrificed with an overdose of pentobarbital sodium (65 mg/kg body weight). The calvarial bone including the cylinders was harvested and fixed with 10% buffered formalin. The specimens were dehydrated using ascending grades of alcohol, infiltrated, and embedded in polyester resin (Rigolac-70F, Rigolac-2004, Nisshin EM) without being decalcified, according to standard procedures.[18] Upon polymerization, these sections were cut in the sagittal direction and ground to a thickness of 50 μm, using the Exakt cutting-grinding system (Exakt). Sections were then stained with 0.1% toluidine blue, and light microscopic images were analyzed (BZ-8000; Keyence).

Histomorphometric Analysis

In the sections of each cylinder, the following parameters were measured: the percentage of area of regenerated tissue, the maximum height of newly formed bone

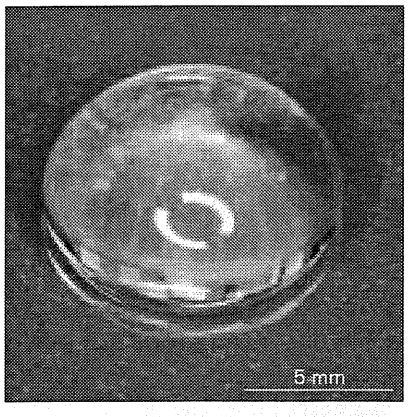

Fig 1 Photograph of 1% PuraMatrix at room temperature. It turns into a gel upon contact with blood.

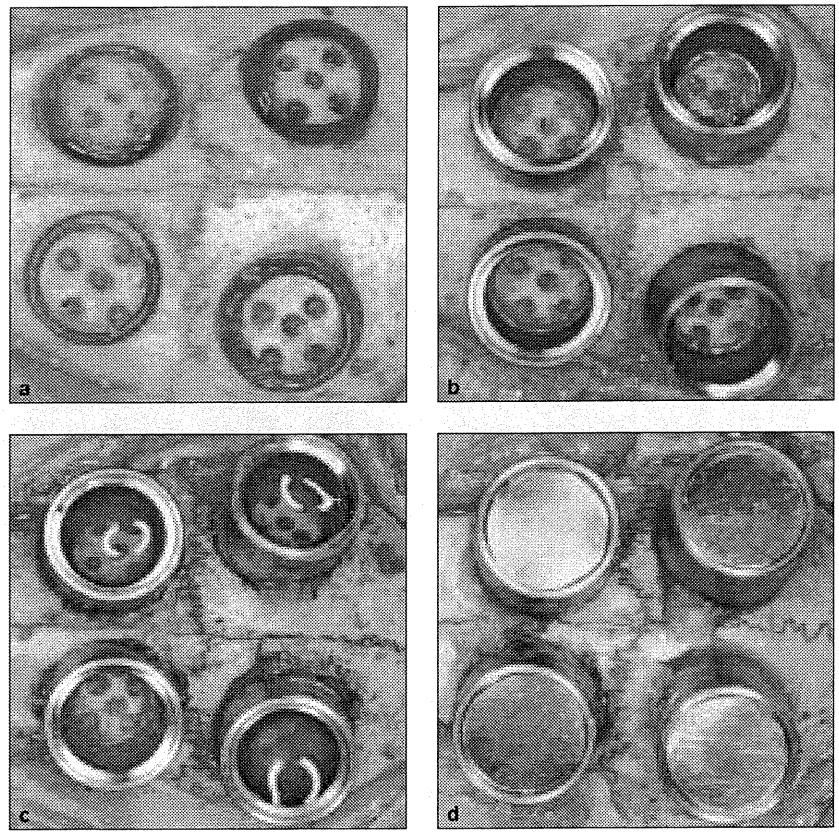

Figs 2a to 2d The surgical procedure. In the left and right parietal and frontal bones, four circular slits were prepared. *(a)* Five holes were prepared in outer cortical bone inside this circle. *(b)* The apical end of the four titanium cylinders was pressed into each slit, and primary fixation was obtained. *(c)* Four titanium cylinders were filled with respective materials. *(d)* The cylinders were covered with a titanium lid.

above the surface of outer cortical bone, and the percentage of area of newly formed bone. Measurements were carried out directly in the digital images at a magnification of ×10. Thereafter, pixel number of each area in the cylinder was counted with an image-processing program (Image J, US National Institutes of Health). Measurements were made as follows: area of regenerated tissue (%) = (pixel number of area of regenerated tissue/total pixel number in the cylinder) × 100; area of newly formed bone (%) = (pixel number of area of newly formed bone/total pixel number in the cylinder) × 100.

STATISTICAL ANALYSIS

Mean values and standard deviations were calculated for the area of regenerated tissue, the maximum height of newly formed bone, and the area of newly formed bone in the cylinders. For statistical analysis, one-way analysis of variance (ANOVA) and a subsequent pairwise one-way ANOVA Tukey significant difference test (SPSS 18.0; SPSS Inc) were used. A value of $P < .05$ was considered to be statistically significant.

RESULTS

During the experiment, all animals showed uneventful healing in the surgical area. There was no reduction in body weight and no postoperative infection in any animals. All cylinders were found to be stable at the time of sacrifice.

Both bone and connective tissue had formed in the cylinders of all groups (Fig 3a). The fitted bases of all cylinders were clearly visible on the histologic specimens and were well integrated into the outer cortical bone of the calvaria. New bone formation seemed to occur from the calvarial bone through the perforations in the outer cortical bone; newly formed bone was also observed in all groups. Under higher magnification, newly formed bone, including cells and some blood vessels, was observed in the connective tissue in the cylinder (Fig 3b). The edges of bone were lined with osteoblast-like cells in the cylinder (Fig 3c). Regenerated tissue in the control cylinder was observed in fewer than one third of the cylinders (Fig 4a). On the other hand, regenerated tissue was observed in about half of the cylinders that had been filled with

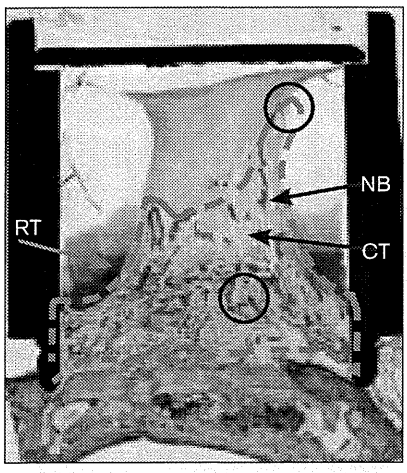

Fig 3a Histologic section of a cylinder stained with toluidine blue (original magnification ×10). RT = area of regenerated tissue; NB = newly formed bone; CT = connective tissue.

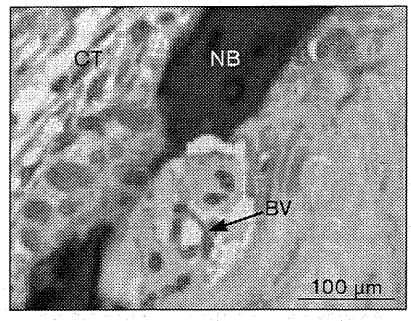

Fig 3b Higher magnification of the circled area in the upper part of Fig 3a (original magnification ×100). CT = connective tissue; NT = newly formed bone; BV = blood vessel.

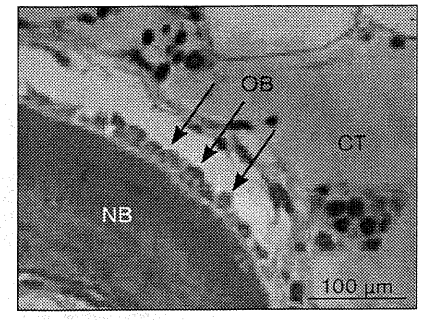

Fig 3c Higher magnification of the circled area in the lower part of Fig 3a (original magnification ×100). NB = newly formed bone; CT = connective tissue; OB = osteoblast-like cells.

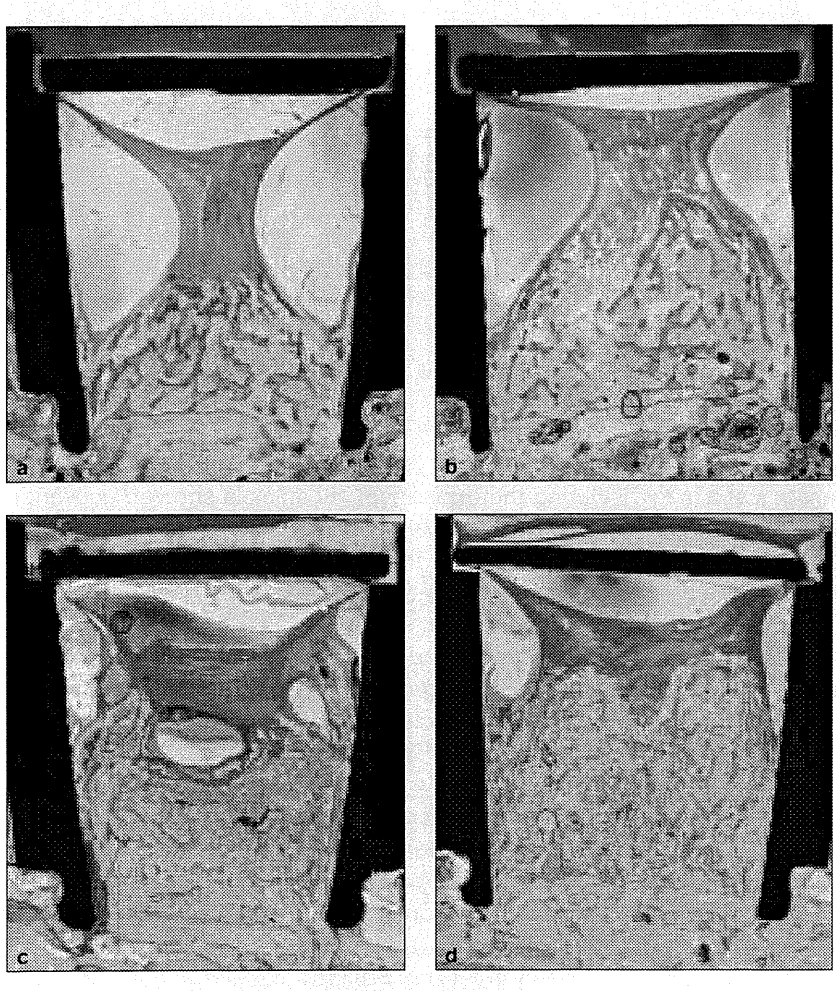

Fig 4 Histologic sections of *(a)* cylinders with empty control, *(b)* rhBMP-2, *(c)* PM, and *(d)* PM/rhBMP-2 (toluidine blue; original magnification ×10).

rhBMP-2 or PM (Figs 4b and 4c). Regenerated tissue in the sample treated with PM/rhBMP-2 was observed in about two thirds of the cylinders (Fig 4d).

Quantitative histomorphometry by image analysis showed that the area of regenerated tissue in the cylinder with PM/rhBMP-2 was significantly increased compared to the empty control ($P < .05$; Fig 5, Table 1).

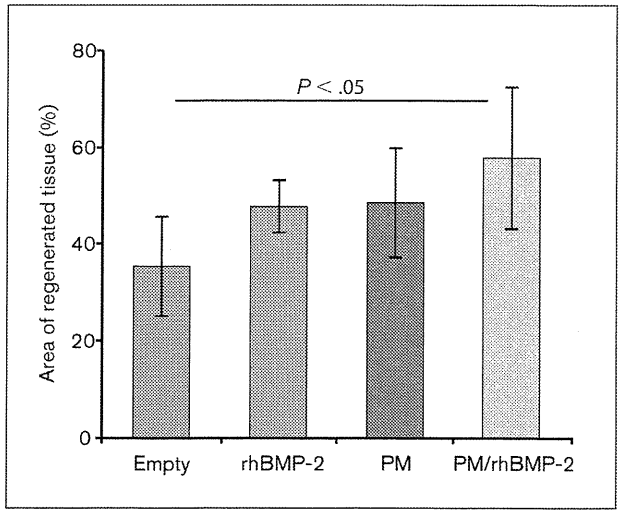

Fig 5 Area of regenerated tissue measured by image analysis. The percentage of area of regenerated tissue in the cylinder in each group ([pixel number of area of regenerated tissue/total pixel number in the cylinder] × 100) is displayed. Bar = SD. ANOVA, PM/rhBMP-2 versus empty control, $P < .05$.

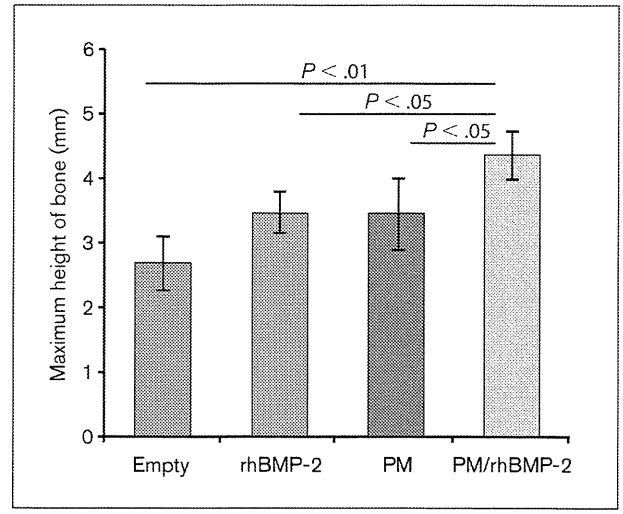

Fig 6 Maximum height of newly formed bone above the surface of the outer cortical bone. The maximum height of newly formed bone in the cylinder with each group is displayed. Bar = SD. ANOVA, PM/rhBMP-2 versus empty control, $P < .01$; PM/rhBMP-2 versus PM or rhBMP-2, $P < .05$.

Fig 7 Newly formed bone area measured by image analysis. The percentage of area of newly formed bone in the cylinder with each group ([pixel number of area of newly formed bone/total pixel number in the cylinder] × 100) is displayed. Bar = SD. ANOVA, PM/rhBMP-2 versus empty control, $P < .05$.

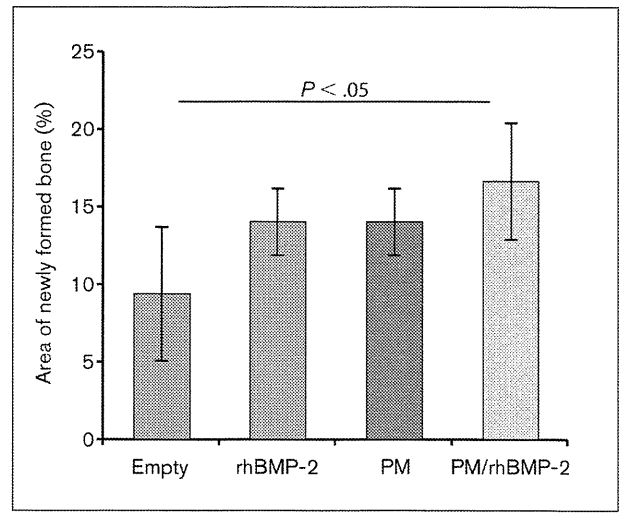

Table 1 Histomorphometric Analysis of Sections in Each Group

Group	No.	Regenerated tissue (%)	Maximum height of bone (mm)	Newly formed bone (%)
Empty	5	35.80 ± 10.35	2.71 ± 0.43	9.39 ± 4.34
rhBMP-2	5	47.94 ± 5.65	3.48 ± 0.32	14.03 ± 2.25
PM	5	48.94 ± 11.33	3.47 ± 0.57	13.99 ± 2.15
PM/rhBMP-2	5	58.06 ± 14.84	4.39 ± 0.39	16.61 ± 3.79

Means and standard deviations shown.

Similarly, the maximum height of newly formed bone in the PM/rhBMP-2 cylinder was significantly increased compared to the empty control ($P < .01$; Fig 6, Table 1). Also, it was significantly increased compared to rhBMP-2 or PM alone ($P < .05$; Fig 6, Table 1). Moreover, the area of newly formed bone in the cylinder with PM/rhBMP-2 was significantly increased compared to the empty control ($P < .05$; Fig 7, Table 1).

DISCUSSION

In the present study, the PM with rhBMP-2 significantly enhanced bone regeneration compared to an unfilled control after 8 weeks. Saline with rhBMP-2 alone did not significantly enhance bone regeneration compared to the control.

Self-assembling peptide hydrogel scaffolds have two main advantages: safety, (ie, there is no risk of microbial transmission), and a structure that resembles the natural extracellular matrix, which has a microstructure to support cell adhesion, migration, proliferation, differentiation, and three-dimensional organization of tissue.[19] In a PM scaffold, bone marrow mesenchymal stem cells can differentiate into mature osteoblasts to form mineralized matrices.[20] Yoshimi et al reported that PM did not enhance bone regeneration in defects of the mandible in dogs, but PM with bone marrow mesenchymal stem cells enhanced bone regeneration.[21] Because PM alone could not enhance bone regeneration, an osteoinductive factor was used in this study.

The lowest possible dose of a signal factor will enhance cost effectiveness in clinical use. The authors preliminarily tested two final concentrations of rhBMP-2—25 μg/mL and 50 μg/mL (data not shown)—and there was no significant difference in newly formed bone. The final concentration of rhBMP-2 (25 μg/mL) was sufficient for bone regeneration in this model. From a clinical point of view, the method in this study may be useful for bone regeneration, because the rhBMP-2 concentration used in the present study is at least 10 times lower than that used in most experimental studies and at least 50 times lower than most clinical studies that have used rhBMP-2 for bone regeneration.[22]

Bone regeneration is expected to be affected by the kinetics of protein release of rhBMP-2 from scaffolds.[23] The binding effect of PM is dependent on the structure and electrostatic charge–induced interactions between the protein and peptide nanofibers. Therefore, protein release through PM is dependent on protein size, the density of the peptide nanofiber, and electrostatic charge. The release kinetics of PM were reported to be rapid in the first 2 hours, to be slower over time, and to reach a plateau after 30 to 50 hours, depending on the protein in the saline solution. Functional protein release was observed to occur over 2 to 3 weeks. PM scaffold is mentioned to be useful for long-term and functional release of active protein.[24–26] The slow and local release of rhBMP-2 may be critical in reducing the concentration to a level that is acceptable for clinical applications. These results indicate that rhBMP-2 had accumulated in the PM before application. Thus, it might have been released at an appropriate time for bone regeneration after application. It was thought that rhBMP-2 could not be maintained in the bone augmentation space, and PM played an important role as a scaffold and drug carrier. With other factors, PM may be expected to play an important role as carrier.

Taken together, the advantages of PM with rhBMP-2 for bone regeneration are expected to include its safety, noninvasiveness, ease of application, and total resorption (absence of residual graft material). Furthermore, an effective dose of rhBMP-2 is expected to be lower with PM than without PM. In addition, this injectable material could provide a further option for bone regeneration in complex areas such as alveolar clefts, bony defects caused by periodontal disease, and the exposed threads of a dental implant. This was a pilot study of PM application with rhBMP-2 using a rabbit calvarial model. Future studies should address the stability of newly formed bone and application in another model, such as augmentation of the maxillary or mandibular ridge.

CONCLUSION

PuraMatrix, a synthetic self-assembling peptide, used in combination with recombinant human bone morphogenetic protein-2 significantly enhanced bone regeneration in a bone augmentation model in rabbits. PuraMatrix promises to be an alternative synthetic material as a useful carrier for recombinant human bone morphogenetic protein for bone regeneration.

ACKNOWLEDGMENTS

The authors thank Drs Akihiro Yajima, Hidenobu Shibuya, Akihito Yamamoto, and Shuhei Tsuchiya for discussion, and the members of the Department of Oral and Maxillofacial Surgery, Nagoya University Graduate School of Medicine, for their assistance and contributions to this study. They also thank 3-D Matrix Ltd, Tokyo, Japan, for providing the PuraMatrix. This work was partly supported by the Japan Society for the Promotion of Science, (19659524, 21659465); and the Global Center of Excellence Program of Nagoya University.

REFERENCES

1. Giannoudis PV, Dinopoulos H, Tsiridis E. Bone substitutes: An update. Injury 2005;36(suppl 3):S20–S27.
2. Voss P, Sauerbier S, Wiedmann-Al-Ahmad M, et al. Bone regeneration in sinus lifts: Comparing tissue-engineered bone and iliac bone. Br J Oral Maxillofac Surg 2009;48:121–126.
3. Goldberg VM, Stevenson S. Natural history of autografts and allografts. Clin Orthop Relat Res 1987;(225):7–16.
4. Pape HC, Evans A, Kobbe P. Autologous bone graft: Properties and techniques. J Orthop Trauma 2010;24(suppl 1): S36–S40.
5. Wiltfang J, Merten HA, Schlegel KA, et al. Degradation characteristics of alpha and beta tri-calcium-phosphate (TCP) in minipigs. J Biomed Mater Res 2002;63:115–121.
6. Bilkay U, Alper M, Celik N, et al. Comparing the osteogenic capacities of bone substitutes: Hydroxyapatite, high-density porous polyethylene, and bone collagen: A biochemical and histological analysis. J Craniofac Surg 2004;15:585–593.
7. Zhang S. Fabrication of novel biomaterials through molecular self-assembly. Nat Biotechnol 2003;21:1171–1178.
8. Zhang S, Gelain F, Zhao X. Designer self-assembling peptide nanofiber scaffolds for 3D tissue cell cultures. Semin Cancer Biol 2005;15:413–420.
9. Bokhari MA, Akay G, Zhang S, Birch MA. The enhancement of osteoblast growth and differentiation in vitro on a peptide hydrogel-polyHIPE polymer hybrid material. Biomaterials 2005;26:5198–5208.
10. Semino CE. Self-assembling peptides: From bio-inspired materials to bone regeneration. J Dent Res 2008;87:606–616.
11. Urist MR. Bone: Formation by autoinduction. Science 1965; 150:893–899.
12. Bessa PC, Casal M, Reis RL. Bone morphogenetic proteins in tissue engineering: The road from laboratory to clinic, part II (BMP delivery). J Tissue Eng Regen Med 2008;2:81–96.
13. Slotte C, Lundgren D, Burgos PM. Placement of autogeneic bone chips or bovine bone mineral in guided bone augmentation: A rabbit skull study. Int J Oral Maxillofac Implants 2003; 18:795–806.
14. Jung RE, Hammerle CH, Kokovic V, Weber FE. Bone regeneration using a synthetic matrix containing a parathyroid hormone peptide combined with a grafting material. Int J Oral Maxillofac Implants 2007;22:258–266.
15. Jung RE, Weber FE, Thoma DS, Ehrbar M, Cochran DL, Hammerle CH. Bone morphogenetic protein-2 enhances bone formation when delivered by a synthetic matrix containing hydroxyapatite/tricalciumphosphate. Clin Oral Implants Res 2008;19:188–195.
16. Zhang S. Emerging biological materials through molecular self-assembly. Biotechnol Adv 2002;20:321–339.
17. Yokoi H, Kinoshita T, Zhang S. Dynamic reassembly of peptide RADA16 nanofiber scaffold. Proc Natl Acad Sci USA 2005;102:8414–8419.
18. Kon K, Shiota M, Ozeki M, Yamashita Y, Kasugai S. Bone augmentation ability of autogenous bone graft particles with different sizes: A histological and micro-computed tomography study. Clin Oral Implants Res 2009;20:1240–1246.
19. Zagris N. Extracellular matrix in development of the early embryo. Micron 2001;32:427–438.
20. Hamada K, Hirose M, Yamashita T, Ohgushi H. Spatial distribution of mineralized bone matrix produced by marrow mesenchymal stem cells in self-assembling peptide hydrogel scaffold. J Biomed Mater Res A 2008;84:128–136.
21. Yoshimi R, Yamada Y, Ito K, et al. Self-assembling peptide nanofiber scaffolds, platelet-rich plasma, and mesenchymal stem cells for injectable bone regeneration with tissue engineering. J Craniofac Surg 2009;20:1523–1530.
22. Smith DM, Cooper GM, Mooney MP, Marra KG, Losee JE. Bone morphogenetic protein 2 therapy for craniofacial surgery. J Craniofac Surg 2008;19:1244–1259.
23. Schmoekel H, Schense JC, Weber FE, et al. Bone healing in the rat and dog with nonglycosylated BMP-2 demonstrating low solubility in fibrin matrices. J Orthop Res 2004;22: 376–381.
24. Nagai Y, Unsworth LD, Koutsopoulos S, Zhang S. Slow release of molecules in self-assembling peptide nanofiber scaffold. J Control Release 2006;115:18–25.
25. Koutsopoulos S, Unsworth LD, Nagai Y, Zhang S. Controlled release of functional proteins through designer self-assembling peptide nanofiber hydrogel scaffold. Proc Natl Acad Sci USA 2009;106:4623–4628.
26. Gelain F, Unsworth LD, Zhang S. Slow and sustained release of active cytokines from self-assembling peptide scaffold. J Control Release 2010;145:231–239.

Effects of the Permeability of Shields with Autologous Bone Grafts on Bone Augmentation

Masayuki Ikeno, DDS[1]/Hideharu Hibi, DDS, PhD[2]/Kazuhiko Kinoshita, DDS, PhD[1]/
Hisashi Hattori, DDS, PhD[3]/ Minoru Ueda, DDS, PhD[4]

Purpose: *The objective of this study was to histologically evaluate and compare the effects of the permeability of shields on bone augmentation in a rabbit calvarial model.* ***Materials and Methods:*** *Twelve adult male Japanese white rabbits were used for the study. Each received four titanium cylinders, which were placed into perforated slits made in the outer cortical bone of the calvaria and filled with autologous iliac bone. The tops of the cylinders were randomly covered with the following test materials:* (1) *uncovered (control),* (2) *a titanium mesh,* (3) *an expanded polytetrafluoroethylene (e-PTFE) membrane, or* (4) *a titanium plate. After 8 weeks, the animals were sacrificed, and ground sections were obtained for histomorphometric analysis.* ***Results:*** *There was no significant difference in augmented bone volume among all groups. However, the distribution of augmented bone in the cylinders differed among the groups. In the uncovered control, there was significantly less augmented bone in the upper third of the cylinder than in the middle or lower thirds. Findings were similar for the titanium mesh group and the e-PTFE membrane group, with significantly less augmented bone in the upper third than in the middle or lower thirds. In the titanium plate group, there was no significant difference in augmented bone among the upper, middle, and lower thirds. The differences among the upper, middle, and lower thirds of the cylinder were smaller in the order of titanium plate, e-PTFE membrane, titanium mesh, and uncovered control.* ***Conclusion:*** *The use of low-permeability shields resulted in small differences in the distribution of bone structure in the present bone augmentation model.* Oral Craniofac Tissue Eng 2011;1:198–204

Key words: *bone augmentation, bone graft, expanded polytetrafluoroethylene membrane, iliac bone, titanium mesh*

Bone augmentation is required prior to dental implant placement if insufficient bone volume is present. Autologous bone grafts have been considered the most effective method for bone augmentation in implant dentistry.[1] In particular, particulate cancellous bone and marrow (PCBM) has often been used in clinical practice as a graft material because it includes osteogenic cells, several growth factors, and mineralized tissue. Grafted PCBM is resorbed, revascularized, and slowly replaced by newly formed bone. However, it initially lacks the intrinsic form and strength to resist external forces. Since PCBM is not sufficiently stable during the healing period, new bone may not form in a grafted site without strong space maintenance. Although clinicians have routinely used resorbable or nonresorbable membranes with PCBM grafts to support bone regeneration, the ideal barrier membrane for the clinical setting is still controversial.

[1]Researcher, Department of Oral and Maxillofacial Surgery, Nagoya University Graduate School of Medicine, Nagoya, Japan.
[2]Associate Professor, Department of Oral and Maxillofacial Surgery, Nagoya University Graduate School of Medicine, Nagoya, Japan.
[3]Lecturer, Department of Oral and Maxillofacial Surgery, Nagoya University Graduate School of Medicine, Nagoya, Japan.
[4]Professor, Department of Oral and Maxillofacial Surgery, Nagoya University Graduate School of Medicine, Nagoya, Japan.

Correspondence to: Dr Hideharu Hibi, Department of Oral and Maxillofacial Surgery, Nagoya University Graduate School of Medicine, 65 Tsuruma-cho, Showa-ku, Nagoya 466-8550, Japan. Fax: +81-52-744-2352. Email: hibihi@med.nagoya-u.ac.jp

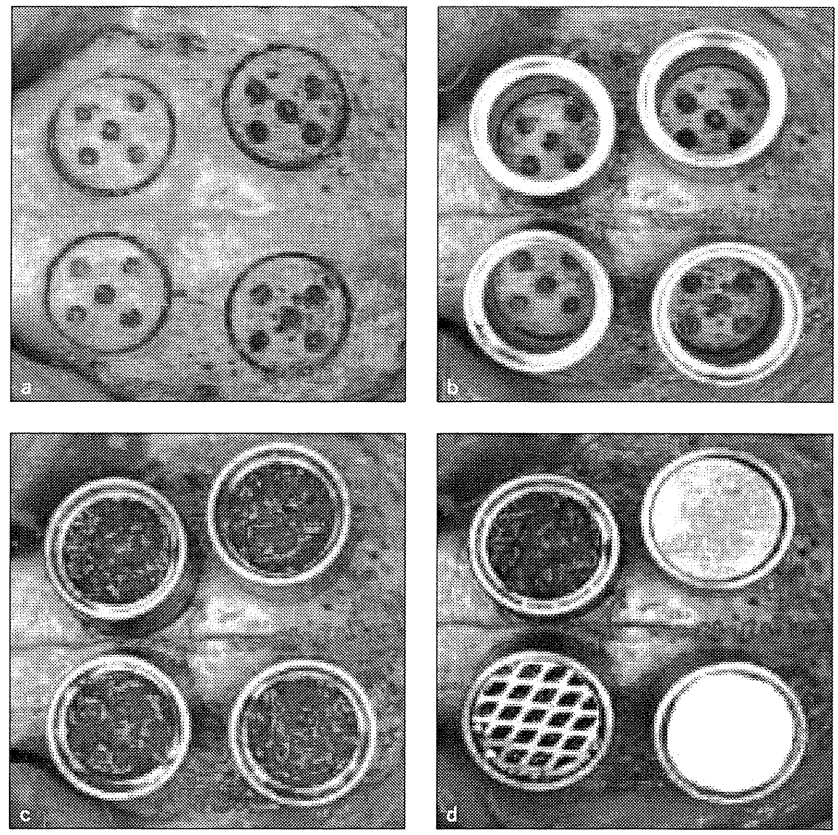

Fig 1 *The surgical procedure.*

Fig 1a In the left and right parietal and frontal bones, four circular slits were prepared. Five holes were prepared in the outer cortical bone inside this circle.

Fig 1b The apical end of each of the four titanium cylinders was pressed into each slit, and primary fixation was obtained.

Fig 1c The four titanium cylinders were filled with PCBM.

Fig 1d The cylinders were covered with the experimental materials (or left uncovered in the control site).

Titanium mesh has been widely used with PCBM grafts, since it is suitable for covering the physiologic shape of the original bone and can facilitate prosthodontic treatment with dental implants.[2] Expanded polytetrafluoroethylene (e-PTFE) membranes have also been used frequently with PCBM, since the combination of PCBM and e-PTFE membranes offers satisfactory clinical results for localized ridge augmentation to allow the placement of dental implants.[3] Both titanium mesh and e-PTFE membranes have been used with PCBM grafts in clinical practice. However, no consensus has been established regarding the differences in regenerated bone underneath them. On the other hand, titanium plates are not preferred for clinical use because of stiffness and lack of permeability. The present authors hypothesized that the quality of augmented bone with PCBM grafts might vary among different coverings because of the differences in permeability among titanium mesh, e-PTFE membrane, and titanium plate. Therefore, the objective of this study was to histologically evaluate and compare the effects of the permeability of shields on bone augmentation in a rabbit calvarial model.

MATERIALS AND METHODS

Animals

Twelve male adult Japanese white rabbits weighing 3.2 to 3.5 kg were used. The animals were kept in individual cages and were fed a standard laboratory diet. General anesthesia was induced by a combination of an intramuscular injection of xylazine (4 mg/kg body weight) and an intravenous injection of pentobarbital sodium (40 to 50 mg/kg body weight) through the ear vein. This experimental protocol was approved by the Animal Experiment Advisory Committee of Nagoya University School of Medicine and was performed in accordance with the Guidelines for Animal Experimentation of Nagoya University.

Surgical Procedure

A midline incision was made from the nasal bone to the sagittal crest, and a cutaneous flap was created. In the left and right parietal and frontal bones, four evenly distributed circular slits were prepared with a trephine drill (Technica) with an inner diameter of 6 mm and a depth of 1 mm. Inside this circle, five evenly distributed holes with a diameter of 1 mm each were prepared with a no. 2 round bur (Fig 1a). The experimental device

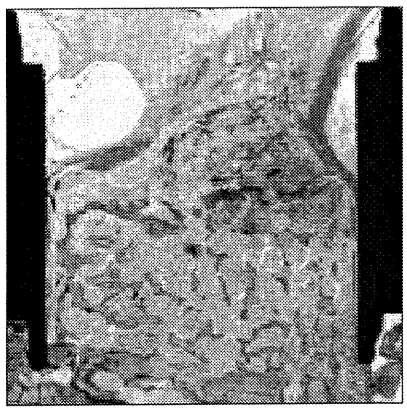

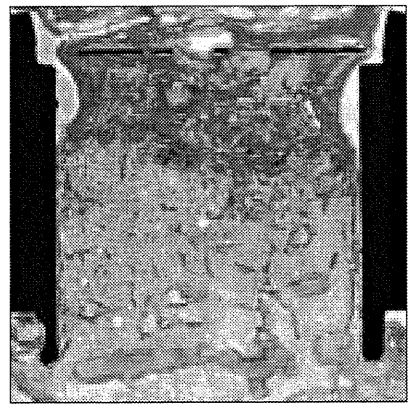

Fig 2 *(Left)* Histologic section of an uncovered control cylinder (toluidine blue; original magnification ×10).

Fig 3 *(Right)* Histologic section of a cylinder covered with titanium mesh (toluidine blue; original magnification ×10).

was a custom-made cylinder of commercially pure titanium (> 99.5% titanium, SPF) with an inner diameter of 6 mm and height of 7 mm. The inside surface of each cylinder was machined titanium. After the bone surfaces of the calvaria were washed with saline to remove any bone powder, the apical end of a titanium cylinder was pressed into each slit (Fig 1b). Each animal received four cylinders, and the cylinders were filled with PCBM harvested from the anterior iliac crest (Fig 1c). The tops of the cylinders were randomly covered with the following: *(1)* uncovered (control), *(2)* a titanium mesh (Stryker Leibinger), *(3)* an e-PTFE membrane (Gore-Tex Japan), or *(4)* a titanium plate (Tokyo Titanium) (Fig 1d). The flaps were adapted and sutured with 4-0 Vicryl (Ethicon) for primary healing. After 8 weeks, the animals were sacrificed and ground sections were obtained for histomorphometric analyses.

Histologic Preparation

The animals were sacrificed with an overdose of pentobarbital sodium (65 mg/kg body weight). The calvarial bone including the cylinders was harvested and fixed with 10% buffered formalin. The specimens were dehydrated using ascending grades of alcohol, infiltrated, and embedded in polyester resin (Rigolac-70F, Rigolac-2004, Nisshin EM) without being decalcified, according to standard procedures.[4] Upon polymerization, these sections were cut in the sagittal direction and ground to a thickness of 50 μm using the Exakt Cutting-Grinding System (Exakt). Sections were then stained with 0.1% toluidine blue and analyzed under a light microscope (BZ-8000, Keyence).

Histomorphometric Analysis

In the sections of each cylinder, the percentage of area of augmented bone was measured. Measurements were carried out directly on the digital images at a magnification of ×10. Thereafter, the pixel number of each area in the cylinder was counted with an image-processing program (ImageJ, US National Institutes of Health). The area of augmented bone (%) was calculated with the following equation: area (%) = (pixel number of area of bone/total pixel number in the cylinder) × 100.

Statistical Analysis

Mean values and standard deviations were calculated for the area of augmented bone in the cylinders. All values were displayed for analysis, including the median. The Kruskal-Wallis test (SPSS 18.0, IBM) was used to identify significant differences and the Mann-Whitney *U* test (SPSS 18.0, IBM) was used for confirmation of significance between groups. A value of $P < .05$ was considered to be statistically significant.

RESULTS

During the experiment, all animals healed uneventfully in the surgical area. There were no reductions in body weight and no postoperative infections in any animals. At the time of sacrifice, 39 of 48 cylinders remained stable in the position placed. However, nine cylinders that were loose were excluded from further analysis (two in the uncovered control group, two in the titanium mesh group, three in the e-PTFE membrane group, and two in the titanium plate group).

The histologic specimens revealed variable patterns of bone formation in the four treatment groups. The fitted bases of all cylinders were clearly visible on the specimens and appeared to be well integrated with the outer cortical bone of the calvaria. Bone formation was observed inside the cylinders but not outside the cylinders, including around the cylinder wall. The augmented tissue consisted of bone with a cancellous structure and connective tissue on the upper surface in all the cylinders. In the control group, augmented bone was mostly observed in the lower half of the cylinder, with fibrous connective tissue evident in the upper half (Fig 2). In the titanium mesh group, the extent of the augmented bone varied from the lower third to the upper third of the cylinders (Fig 3).

Fig 4 *(Left)* Histologic section of a cylinder covered with e-PTFE membrane (toluidine blue; original magnification ×10).

Fig 5 *(Right)* Histologic section of a cylinder covered with a titanium plate (toluidine blue; original magnification ×10).

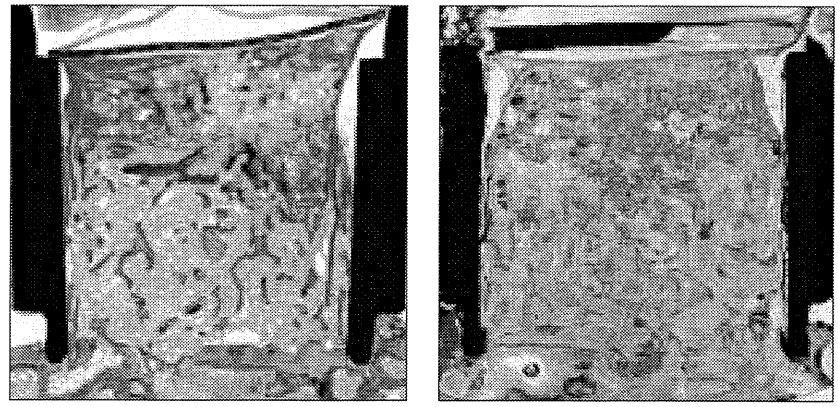

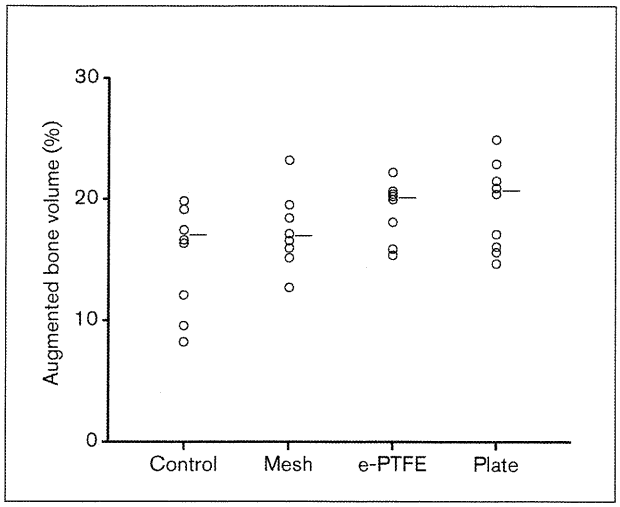

Fig 6 Area percentages of augmented bone measured by image analysis. The percentage of area of augmented bone in the cylinder in each group ([pixel number of area of augmented bone/total pixel number in the cylinder] × 100) is displayed. The lines to the right of the circles indicate the median values. No significant differences were observed among the groups.

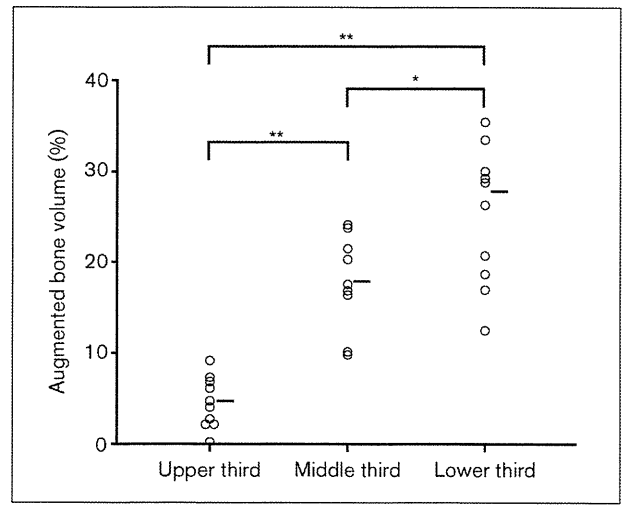

Fig 7 Area percentages of augmented bone in specific areas in the cylinders of the uncovered control group. The lines to the right of the circles indicate median values. Significant differences were seen between the three areas in the cylinder (Kruskal-Wallis test; $P < .01$). *$P < .05$; **$P < .01$ (Mann-Whitney U test).

Table 1 Augmented Bone Volume (%, Means ± Standard Deviations) of the Cylinders

Group	n	Upper third	Middle third	Lower third	Average
Control	10	4.55 ± 2.81	17.79 ± 4.97	25.21 ± 7.60	15.85 ± 4.32
Mesh	10	10.69 ± 5.44	21.37 ± 6.11	19.36 ± 8.13	17.14 ± 2.85
e-PTFE	9	14.14 ± 5.03	22.01 ± 2.91	20.99 ± 3.55	19.05 ± 2.30
Plate	10	16.29 ± 3.91	22.34 ± 5.93	19.93 ± 7.16	19.52 ± 3.42

A similar appearance was observed in both the e-PTFE membrane group (Fig 4) and the titanium plate group (Fig 5). The largest amount of augmented bone in the upper third of the cylinder was observed in the titanium plate group.

Quantitative histomorphometric analysis revealed that the content of augmented bone was similar in all groups. There was no significant difference in augmented bone volume among all groups (Fig 6, Table 1). However, the augmented bone volumes found in the upper, middle, and lower thirds of the cylinders were clearly different within each group. In the uncovered control group, augmented bone volume in the upper third (4.55% ± 2.81%) of the cylinder was significantly lower than that seen in the middle (17.79% ± 4.97%) and lower (25.21% ± 7.60%) thirds (Fig 7, Table 1). In the titanium mesh group, augmented bone volume in the upper third (10.69% ± 5.44%) of the

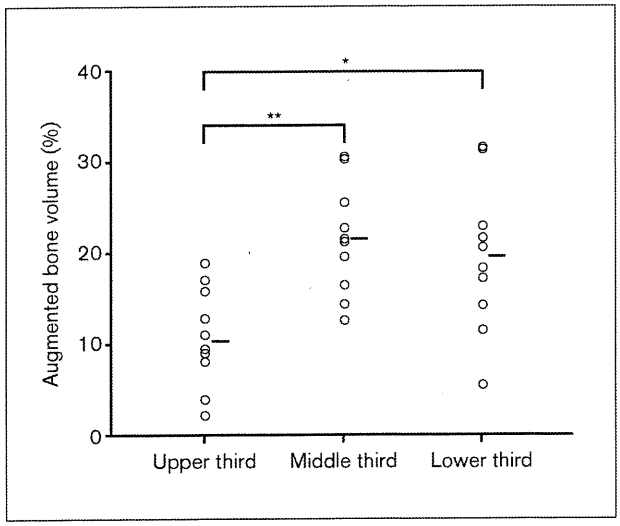

Fig 8 Area percentages of augmented bone in specific areas in the cylinders of the titanium mesh group. The lines to the right of the circles indicate median values. Application of the Kruskal-Wallis test revealed a significant difference among the three areas in the cylinder ($P < .01$). Mann-Whitney U test: $^*P < .05$; $^{**}P < .01$.

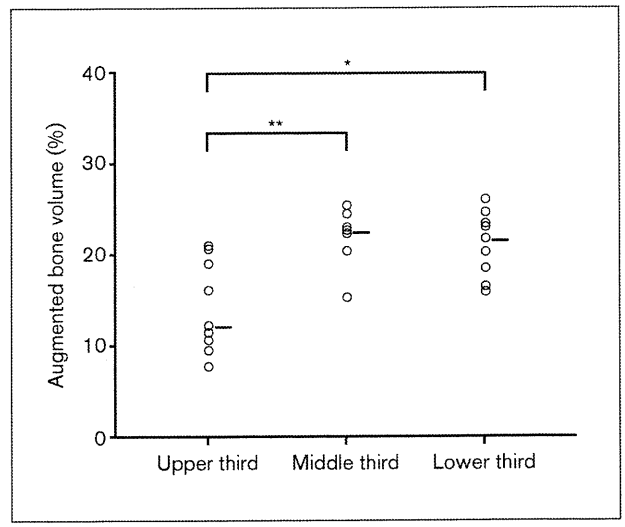

Fig 9 Area percentages of augmented bone in specific areas in the cylinders of the e-PTFE membrane group. The lines to the right of the circles indicate the median values. Significant differences were seen among the three areas in the cylinder (Kruskal-Wallis test; $P < .01$). Significant differences between areas, as determined by the Mann-Whitney U test: $^*P < .05$; $^{**}P < .01$.

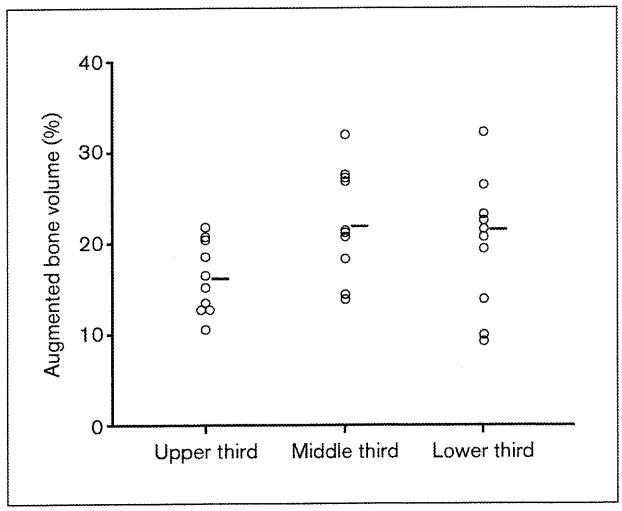

Fig 10 Area percentages of augmented bone of specific areas in the cylinders of the titanium plate group. The lines to the right of the circles indicate the median values. No significant differences among the three areas were observed.

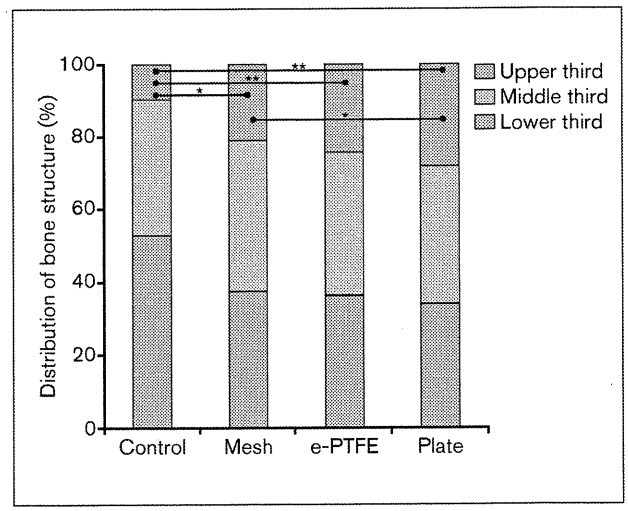

Fig 11 Distribution of bone structure in the four groups. Application of the Kruskal-Wallis test revealed a significant difference among the three areas in the cylinder ($P < .01$). Significant differences between areas, as determined by the Mann-Whitney U test: $^*P < .05$; $^{**}P < .01$.

cylinder was significantly lower than that in the middle (21.37% ± 6.11%) and lower (19.36% ± 8.13%) thirds (Fig 8, Table 1). Similarly for the e-PTFE membrane group, augmented bone volume in the upper third (14.14% ± 5.03%) of the cylinder was significantly smaller than that observed in the middle (22.01% ± 2.91%) and lower (20.99% ± 3.55%) thirds (Fig 9, Table 1). In contrast, in the titanium plate group, there were no significant differences in augmented bone volume between the upper (16.29% ± 3.91%), middle (22.34% ± 5.93%), and lower (19.93% ± 7.16%) thirds of the cylinder (Fig 10, Table 1). The distribution of bone structure differed significantly between the groups, with the differences between the upper, middle, and lower thirds being smaller in the order of titanium plate, e-PTFE membrane, titanium mesh, and uncovered control (Fig 11).

DISCUSSION

The purpose of the present study was to histologically evaluate bone quality following augmentation with autologous PCBM and covering the augmented sites with three different nonresorbable shields. The newly formed tissue in the present model consisted of small amounts of mineralized bone and bone marrow space. In the uncovered control group, the upper third of the cylinder was penetrated by connective tissue from the surrounding area. Therefore, the PCBM, including osteogenic cells, was pressed into the lower portion of the grafted zone, and the newly augmented bone was increased in the lower third. These aspects decreased in the order of titanium mesh, e-PTFE membrane, and titanium plate because the shields were progressively more able to prevent the ingrowth of connective tissue. The titanium plate used in this study was expected to effectively prevent the ingrowth of fibrous tissue because of its lower sensitivity to pressure and micromotion than the other shields, so that the most augmented bone might be formed in the titanium plate group. The surrounding soft tissue penetration and micromotion were reported as factors inhibiting bone ingrowth in the devices.[5]

Bone regeneration following grafting with PCBM occurs not only because of incorporation of the graft but also through the induction of osteogenesis by the grafted mesenchymal stem cells. The biology of cancellous bone graft repair has three features: *(1)* cancellous grafts are revascularized more rapidly and completely than cortical grafts; *(2)* gradual substitution of cancellous bone initially involves an appositional bone formation phase, followed by a resorptive phase; and *(3)* cancellous grafts tend to repair themselves completely with time.[6] Thus, during the healing period, grafted PCBM requires strong space maintenance to occupy the grafted space.

To improve the current understanding of guided bone augmentation (GBA), numerous animal studies have investigated rabbit calvaria. The skull area offers good surgical access, and the placement of experimental devices is uncomplicated compared to that of mandibular bone, where masticatory forces may lead to the tearing of soft tissue, dislocation of experimental devices, and infection. The bilateral use of the parietal bone was found to be reliable in experimental GBA models with respect to blood supply and bone quality.[7] The titanium cylinder used in the present model, which is less sensitive to pressure and micromotion than silicone materials,[8] effectively prevented the entry of connective tissue cells from the lateral side and the ingrowth of connective tissue. Therefore, it is a suitable means of comparing differences in the shields placed on the upper side of the cylinder. Using a similar experimental model in rabbit calvaria, Schmid et al reported that equal amounts of new bone had formed under both titanium-sealed and e-PTFE membrane–covered devices, thereby confirming that membrane permeability was not necessary for GBA.[9] They also reported that angiogenesis was observed in the devices with total occlusion on the extraskeletal bone.[10] Yamada et al also reported that the total occlusion and sufficient stiffness of the titanium cap allowed predictable mineralized bone augmentation to occur beyond the rabbit skeletal envelope, with angiogenesis originating from cortical bone.[11] Augmented bone requires a blood supply from the cortical bone but not from the surrounding soft tissue. Lundgren et al reported that the space-maintaining properties of a barrier may be at least as important as barrier occlusiveness[12]; the present study supports this finding.

In clinical practice, a titanium mesh or titanium-reinforced (TR) e-PTFE membrane is often used as a barrier over PCBM grafts. These can provide more time for the osteogenic cells to occupy the grafted area before epithelial cells can enter. The structure of the titanium mesh can prevent the migration of epithelial cells to the lower grafted area, while connective tissue ingrowth from outside of the multiporous surface is allowed into the upper grafted area. Therefore, the supply of nutrients and blood is good. In contrast, the structure of the TR e-PTFE membrane can prevent the migration of epithelial cells to the entire grafted area. However, the rigidity of TR e-PTFE membranes has reportedly resulted in an increase in the number of membrane exposures by mucosal perforation when they are used for vertical ridge augmentation.[13] Recently, the use of the TR e-PTFE membrane to cover particulate bone graft in augmentation has led to good results.[14–16] Titanium membranes were introduced to increase the stability of barrier membranes.[17] A commercialized microperforated titanium membrane (FRIOS BoneShield) was evaluated with graft materials in a clinical study.[18,19] The rigidity of the titanium membrane provided good results without exposure, but an increased number of membrane exposures was seen. In 78 procedures, 23 membranes (29%) became exposed because of mucosal perforation. Therefore, careful soft tissue management is required to prevent membrane exposures, since rigid membranes are more difficult to insert than flexible membranes in the clinical setting.

CONCLUSION

The use of low-permeability shields resulted in small differences in the distribution of bone structure in the present bone augmentation model. From the standpoint of the quality of augmented bone, an ideal shield for

particulate cancellous bone and marrow grafts may be a membrane that has sufficient occlusive properties and stiffness but will not become exposed. Further studies should address the stability of augmented bone and the development of an ideal shield for particulate cancellous bone and marrow grafts.

ACKNOWLEDGMENTS

We thank Drs Akihiro Yajima, Akihito Yamamoto, Tomoo Oda, and Shuhei Tsuchiya for their helpful discussions and members of the Department of Oral and Maxillofacial Surgery, Nagoya University Graduate School of Medicine, for their valuable assistance and contributions to this study. This work was partly supported by a Grant-in-Aid for Science Research (19659524, 21659465) from the Ministry of Education, Culture, Sports, Science and Technology of Japan and the Global Center for Excellence Program for Education and Research of Micro-Nano Mechatronics in Nagoya University.

REFERENCES

1. Chiapasco M, Casentini P, Zaniboni M. Bone augmentation procedures in implant dentistry. Int J Oral Maxillofac Implants 2009;24(suppl):237–259.
2. Yamashita Y, Yamaguchi Y, Tsuji M, Shigematsu M, Goto M. Mandibular reconstruction using autologous iliac bone and titanium mesh reinforced by laser welding for implant placement. Int J Oral Maxillofac Implants 2008;23:1143–1146.
3. Buser D, Dula K, Hess D, Hirt HP, Belser UC. Localized ridge augmentation with autografts and barrier membranes. Periodontol 1999;19:151–163.
4. Kon K, Shiota M, Ozeki M, Yamashita Y, Kasugai S. Bone augmentation ability of autogenous bone graft particles with different sizes: A histological and micro-computed tomography study. Clin Oral Implants Res 2009;20:1240–1246.
5. Goodman S, Aspenberg P, Song Y, Regula D, Lidgren L. Intermittent micromotion and polyethylene particles inhibit bone ingrowth into titanium chambers in rabbits. J Appl Biomater 1995;6:161–165.
6. Burchardt H. The biology of bone graft repair. Clin Orthop Relat Res 1983;174:28–42.
7. Slotte C, Lundgren D, Sennerby L. Bone morphology and vascularization of untreated and guided bone augmentation-treated rabbit calvaria: Evaluation of an augmentation model. Clin Oral Implants Res 2005;16:228–235.
8. Slotte C, Lundgren D, Burgos PM. Placement of autogeneic bone chips or bovine bone mineral in guided bone augmentation: A rabbit skull study. Int J Oral Maxillofac Implants 2003; 18:795–806.
9. Schmid J, Hämmerle CH, Olah AJ, Lang NP. Membrane permeability is unnecessary for guided generation of new bone. An experimental study in the rabbit. Clin Oral Implants Res 1994;5:125–130.
10. Schmid J, Wallkamm B, Hämmerle CH, Gogolewski S, Lang NP. The significance of angiogenesis in guided bone regeneration. A case report of a rabbit experiment. Clin Oral Implants Research 1997;8:244–248.
11. Yamada Y, Tamura T, Hariu K, Asano Y, Sato S, Ito K. Angiogenesis in newly augmented bone observed in rabbit calvarium using a titanium cap. Clin Oral Implants Res 2008; 19:1003–1009.
12. Lundgren AK, Sennerby L, Lundgren D. Guided jaw-bone regeneration using an experimental rabbit model. Int J Oral Maxillofac Surg 1998;27:135–140.
13. Jovanovic SA, Schenk RK, Orsini M, Kenney EB. Supracrestal bone formation around dental implants: An experimental dog study. Int J Oral Maxillofac Implants 1995;10:23–31.
14. Lindfors LT, Tervonen EA, Sándor GK, Ylikontiola LP. Guided bone regeneration using a titanium-reinforced ePTFE membrane and particulate autogenous bone: The effect of smoking and membrane exposure. Oral Surg Oral Med Oral Pathol Oral Radiol Endod 2010;109:825–830.
15. Merli M, Lombardini F, Esposito M. Vertical ridge augmentation with autogenous bone grafts 3 years after loading: Resorbable barriers versus titanium-reinforced barriers. A randomized controlled clinical trial. Int J Oral Maxillofac Implants 2010;25:801–807.
16. Urban IA, Jovanovic SA, Lozada JL. Vertical ridge augmentation using guided bone regeneration (GBR) in three clinical scenarios prior to implant placement: A retrospective study of 35 patients 12 to 72 months after loading. Int J Oral Maxillofac Implants 2009;24:502–510.
17. Lundgren D, Lundgren AK, Sennerby L, Nyman S. Augmentation of intramembranous bone beyond the skeletal envelope using an occlusive titanium barrier. An experimental study in the rabbit. Clin Oral Implants Res 1995;6:67–72.
18. Kim YK, Yun PY, Kim SG, Oh DS. In vitro scanning electron microscopic comparison of inner surface of exposed and unexposed nonresorbable membranes. Oral Surg Oral Med Oral Pathol Oral Radiol Endod 2009;107:e5–11.
19. Watzinger F, Luksch J, Millesi W, et al. Guided bone regeneration with titanium membranes: A clinical study. Br J Oral Maxillofac Surg 2000; 38:312–315.

Bone Regeneration with Self-Assembling Peptide Nanofiber Scaffolds in Tissue Engineering for Osseointegration of Dental Implants

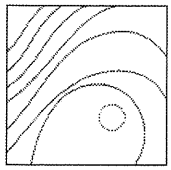

Tomoyuki Kohgo, DDS[1]/Yoichi Yamada, DDS, PhD[2]/Kenji Ito, DDS, PhD[3]
Akihiro Yajima, DDS, PhD[4]/Ryoko Yoshimi, DDS[5]/Kazuto Okabe, DDS[5]
Shunsuke Baba, DDS, PhD[6]/Minoru Ueda, DDS, PhD[7]

The aim of this study was to evaluate the correlation between the osseointegration of dental implants and tissue-engineered bone using a nanofiber scaffold, PuraMatrix (PM). The first molar and all premolars in the mandibular regions of dogs were extracted, and three bone defects were prepared with a trephine bur on both sides of the mandible after 4 weeks. The experimental groups were as follows: (1) *PM,* (2) *PM and dog mesenchymal stem cells (dMSCs),* (3) *PM, dMSCs, and platelet-rich plasma, and* (4) *control (defect only). Implants were placed in the prepared areas 8 weeks later and were assessed by histologic and histomorphometric analyses (bone-to-implant contact [BIC]). The BICs for groups 1, 2, 3, and 4 were 40.77%, 50.35%, 55.64%, and 30.57%, respectively. The findings indicate that PM may be useful as a scaffold for bone regeneration around dental implants.* (Int J Periodontics Restorative Dent 2011;31:e9–e16.)

[1]Department of Oral and Maxillofacial Surgery, Nagoya City University School of Medical Sciences, Nagoya, Japan; Formerly, Student, Department of Oral and Maxillofacial Surgery, Nagoya University Graduate School of Medicine, Nagoya, Japan.
[2]Assistant Professor, Center for Genetic and Regenerative Medicine, Nagoya University Graduate School of Medicine, Nagoya, Japan.
[3]Assistant Professor, Department of Clinical Cell Therapy and Tissue Engineering, Nagoya University School of Medicine, Nagoya, Japan.
[4]Chief, Department of Oral and Maxillofacial Surgery, Hoshigaoka Maternity Hospital, Nagoya, Japan.
[5]Student, Department of Oral and Maxillofacial Surgery, Nagoya University Graduate School of Medicine, Nagoya, Japan.
[6]Chief, Department of Regenerative Medicine, Institute of Biomedical Research and Innovation, Kobe, Japan.
[7]Professor and Chair, Department of Oral and Maxillofacial Surgery, Nagoya University Graduate School of Medicine, Nagoya, Japan.

Correspondence to: Dr Yoichi Yamada, 65 Tsuruma-cho, Showa-ku, Nagoya 466-8550, Japan; fax: +81-52-744-2352; email: yyamada@med.nagoya-u.ac.jp.

Bone regeneration and augmentation for dental implant placement are frequently carried out using autografts, allografts, xenografts, or synthetic materials.[1–4] Among these materials, autogenous bone grafts are considered an ideal graft material and the gold standard. However, the harvesting of bone grafts injures otherwise healthy sites, causing morbidity.[5,6] Presently, bone substitutes such as hydroxyapatite, tricalcium phosphate, or inorganic porous animal-derived bone minerals[7–9] are used to provide alternatives to autogenous bone for improvement of the bone volume; these materials need to be researched more regarding their safety and effectiveness in clinical practice.[10,11] Moreover, these materials and internal structures may not provide a particularly favorable environment for cell survival and bone regeneration, and the microscale environment of these materials needs to serve as an extracellular matrix (ECM) in nature.

The present study considered the use of the novel matrix material PuraMatrix (PM; 3-D Matrix),

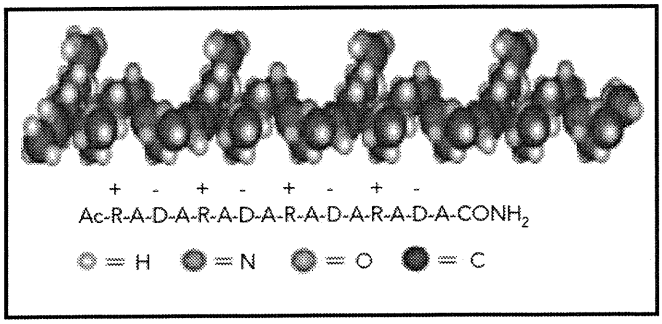

Fig 1 *Molecular structure of PM. Molecular models of the amphiphilic self-complementary peptide have 16 amino acids with an alternating polar and nonpolar pattern. A = alanine; R = arginine; D = aspartic acid; + and – refer to the positively and negatively charged residues, respectively.*

which is synthesized by chemical peptide methods, has similarities to the fibers and pore sizes found in ECM, is not animal-derived, and shows fluid characteristics.[12] Therefore, PM exhibits good plasticity, absorption, biocompatibility properties, and is devoid of animal-derived pathogens and antigens.[5]

Recently, a concept of tissue engineering whereby isolated cells, signal molecules, and scaffolds are necessary for tissue regeneration has been proposed.[13] Successful tissue engineering involves the implantation of living cells along with synthetic materials and results in new tissue regeneration.[14] Tissue engineering procedures for bone augmentation offer significant advantages compared with conventional grafts since there is minimal or little donor site morbidity.[15] Within this concept, the authors suggest the use of mesenchymal stem cells (MSCs) as the cells, platelet-rich plasma (PRP) as the source of signal molecules,[16] and PM as the scaffold. Generally, in tissue engineering, the cells are typically seeded in a three-dimensional (3D) scaffold, which not only provides the anchorage for cell adhesion, but also creates a suitable cellular microenvironment through adhesions that regulate cell differentiation and cell-cell signaling.[13]

Method and materials

All animal experiments undertaken were performed in strict accordance with protocols approved by the Institutional Animal Care Committee. After a period of acclimation, hybrid dogs with a mean age of 2 years were operated on under general anesthesia. The first molar and all premolars in the mandible were extracted, and extraction sites were allowed to heal for 4 weeks. Bone defects on both sides of the mandible were prepared with a 10-mm (diameter and depth) trephine bur.[17–19] The defects received implants using graft materials as follows: group 1, PuraMatrix (PM); group 2, PM and dog MSCs (dMSCs; PM/dMSCs); group 3, PM, dMSCs, and PRP (PM/dMSCs/PRP); and group 4, control (defect only). Without any differences between the various sites in terms of bone healing, three defects per side of the mandible were prepared, and the four groups of materials were implanted in a random and non–site-specific manner. After 8 weeks, bone biopsies were taken using a 2-mm-diameter trephine bur, and Brånemark implants (8.5 mm in length, 3.75 mm in diameter; Nobel Biocare) were placed into the bone regeneration areas.

Cell cultivation

Bone marrow cell isolation and expansion were performed according to previous methods.[14] The cells were incubated at 37°C in a humidified atmosphere containing 95% air and 5% carbon dioxide. In culture, dMSCs were trypsinized and used for implanting.

PM is a synthetic peptide consisting of a sequence of 16 amino acids (Ac-RADARADARADARADA-$CONH_2$) (Fig 1). PM peptide hydrogel was sonicated for 30 minutes using a sonic machine (Branson). Phosphate-buffered saline (100 μL) was layered over the top of the hydrogel, allowed to sit at room temperature for 1 minute, and then mixed gently. PRP was prepared according to previous methods.[17] Then, the PRP and dMSCs (1.0×10^7 cells/mL) or dMSCs alone (1.0